10. Nanostructures of Common Metals

Melinda Mohl, Krisztián Kordás

Since nanosized metals with magnetic features, and porous and noble metals, are discussed in other chapters of this handbook, here we present a complementary, comprehensive review on other metal nanostructures. Accordingly, this chapter is devoted to review the strategies of synthesis as well as properties of the most common transition- and post-transition-metal nanoparticles. Particular attention is paid to scalable production methods and enabled or foreseen applications of such metals, including low-melting-point lead, bismuth, tin, and indium, some of the refractories including tungsten, molybdenum, tantalum, and titanium, as well as a few more of the very commonly used metals such as copper, aluminum, and zinc. The review is expected to help the readers to get a glance at the state-of-the-art in the field and to foster new studies to overcome challenges associated typically with controlled bulk production and exploitation of this family of nanomaterials.

Looking at the Periodic Table of elements, we find about 80 natural/stable isotopes of metals that are nonmagnetic and nonprecious. Among these, the alkali and alkali-earth metals (s-group) are extremely reactive, and the lanthanoids and actinoids (f-group) and some of the d-group metals are of low abundance, leaving roughly 20 elements that can be considered as practical choices for large-scale industrial use in metallic form, especially when talking about nanoparticles. Though each metal has its peculiarities, the basic rules concerning their size-dependent physical properties follow the general trends observed when talking about nanosized structures of other metals. Small crystal size can result in: increased chemical reactivity due to the relatively large number of surface atoms and vacancies at specific crystal edges and apices, melting point depression because of the large surface energy, decreased electrical and thermal conductivity due to the more pronounced electron and phonon scattering at the crystal boundaries, the appearance of molecular-like electronic states instead of the ordinary overlapped valence and conduction bands giving rise to the onset of semiconducting/semimetallic behavior in very small clusters or very thin wires, the appearance of magnetic polarization, etc. [10.1–13].

Since the pioneering work of *Granqvist* and *Buhrman* [10.14], quite some efforts have been devoted to synthesize and study fine metal particles, and to determine how their properties, which may differ from those of their bulk counterparts, could be exploited for the benefit of various industries [10.15–23]. Synthesis methods may be divided into physical and chemical routes. Within these, we can further distinguish crystal growth with or without a template. The common feature in most of these methods is how the nanoparticles form:

1. Decomposition/reduction of precursor material or evaporation of metal atoms/clusters,
2. Formation of nuclei, and finally
3. Nanocrystal growth.

R. Vajtai (Ed.), *Springer Handbook of Nanomaterials*, DOI 10.1007/978-3-642-20595-8_10,

In this chapter, we select 11 metals – aluminum, bismuth, copper, indium, lead, molybdenum, tantalum, tin, titanium, tungsten, and zinc – which we consider as the most relevant ones, and present a review on their synthesis and applications reported in the open literature.

10.1 Post-Transition Metals

Metals of the p-block elements – and in some classifications also Zn, Cd, and Hg – belong to the category of post-transition metals. Though the chemical properties of p-block metals can be very different due to the rapid decrease of their metallic character with decreasing number of periods and increasing group number, common features of these metals are their low melting point, ductility, and moderate electrical as well as thermal conductivity (except for aluminum, which has superior electron and phonon transport behavior compared with most of the metals in the entire Periodic Table of elements). In Sect. 10.1, we consider lead, bismuth, tin, indium, and aluminum, as the most frequently applied metals of the p-block elements with reasonable potential in future nanodevices [10.24, 25].

10.1.1 Lead, Bismuth, Tin, and Indium

Lead, bismuth, tin, and indium, typically known for their low melting point, ductility, and good wetting by other metals, are all predestined to be excellent soldering materials. Owing to their low Young's moduli ($E_{Pb} = 14.0\,GPa$, $E_{Bi} = 31.7\,GPa$, $E_{Sn} = 41.4\,GPa$, and $E_{In} = 12.7\,GPa$) [10.26] compared with other ordinary metals (e.g., $E_{Cu} = 110\,GPa$, $E_{Al} = 68.0\,GPa$, and $E_{W} = 400\,GPa$), soft mechanical bonds are enabled and used in sealing, plumbing, as well as (solid-state) lubrication. The electrical properties, which depend also on the crystal size of these materials, also have some peculiarities. Lead has a relatively high superconductivity-transition temperature ($T_c \approx 6\,K$ [10.27, 28], one of the highest values among pure metals). Bismuth has a very high thermoelectric coefficient ($S \approx -30$ to $60\,\mu V/K$ [10.29, 30], depending on crystal size) and large mean free path of carriers [10.31–36], and shows semiconducting behavior on the nanoscale [10.37–39], suggesting applications in novel electronic devices. Although many studies deal with the superconducting behavior of nanowires of tin and indium, demonstrating shape- and size-dependent [10.40–42] properties [10.43,44], real applications of these nanostructured metals are mainly related to lead-free electronics packaging [10.45], catalysis [10.46], and batteries [10.47], although they are also used as a sacrificial template for galvanic exchange plating [10.48] or as a starting material of the widely used tin and indium oxides and other compounds. Accordingly, a large number of different methods have been developed to generate both Pb [10.49–64] and Bi [10.31–36, 65–76] nanostructures of various shapes and sizes [10.49–56].

Lee and coworkers recently demonstrated a vapor condensation method to synthesize zero-dimensional Pb nanoparticles by evaporating high-purity lead in Ar atmosphere at 0.1–2 Torr pressure [10.57]. The particles were collected by thermophoresis using a steel plate cooled with liquid nitrogen. The mean size of the nanoparticles could be varied from 4.5 to 86 nm. Another useful route leading to nanoparticles was developed by *Dang* et al., in which a surfactant-assisted solution-phase approach was applied to generate nanoparticles with average diameter of 40 nm [10.53]. First, Pb granules were dispersed in stearic acid containing paraffin oil at 330 °C. Small droplets of lead were generated by a stirring force, immediately reacting with stearic acid to form a lead stearate layer around the droplet. Tribological measurements of the nanoparticles dispersed in paraffin oil showed that, even at very low concentration, the antiwear performance was markedly improved.

In a set of publications [10.49, 50], *Xia* and coworkers demonstrated a bottom-up approach for chemical synthesis of Pb spherical colloids by thermal decomposition of lead acetate in the presence of tetra(ethylene glycol) (TEG) and poly(vinyl pyrrolidone) (PVP). Large quantities of single-crystal Pb nanowires [10.54, 58] (Fig. 10.1a) can be obtained under conditions similar to in the aforementioned approach; however, the reaction must be performed in ethylene glycol. In comparison with the evolution of face-centered cubic (fcc) metal nanowires, ethylene glycol here only serves as a high-boiling-point solvent to facilitate thermal decomposition of the precursor, while the major function of PVP is to prevent Pb nanoparticles from aggregating in the nucleation stage. The growth mechanism (Fig. 10.1c,d)

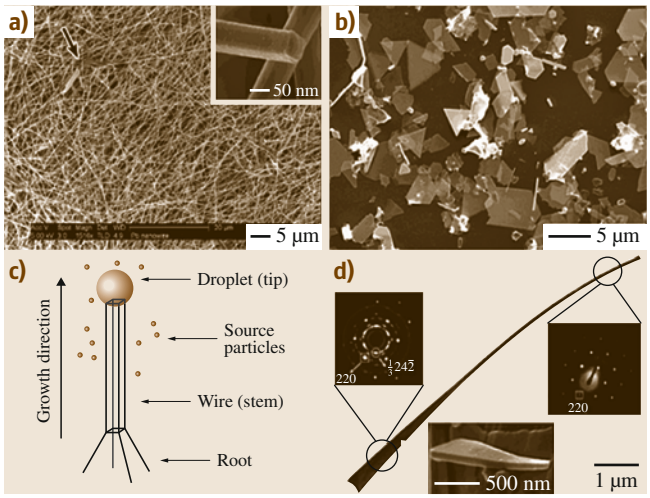

Fig. 10.1 **(a)** Scanning electron microscopy (SEM) image of Pb nanowires prepared in ethylene glycol in the presence of PVP. *Inset* shows the rectangular cross-section of the nanowires. **(b)** SEM image of hexagonal and triangular flakes of Pb synthesized by increasing the amount of PVP. **(c)** Schematic image of the presumed mechanism for nanowire growth. **(d)** Transmission electron microscopy (TEM) image of a growing nanowire; *insets* show selected-area electron diffraction (SAED) patterns of its root and stem. (After [10.58]) ▶

of these nanowires is believed to be a combination of the solution–liquid–solid (SLS) [10.59] method and the Ostwald ripening phenomenon. In addition to nanoparticles and nanowires, Pb hexagonal and triangular nanoprisms (Fig. 10.1b) have also been reported [10.55, 58]. The preparation of thin plates (thickness $< 100\,\text{nm}$) is based on a kinetically controlled polyol process.

Another useful route to synthesize one-dimensional nanostructures is to load materials into the channels of porous membranes such as track-etched polycarbonate (PTCE), anodic aluminum oxide (AAO) or mesoporous silica membranes (e.g., MCM-41, SBA-15). Loading of these porous structures can be achieved by a wide variety of techniques, such as liquid-phase injection, vapor-phase sputtering, and chemical or electrochemical deposition. Besides porous mesoscopic membranes, crystal surfaces with specific steps and edges may also be used as templates for self-ordering nanoparticles [10.60–64]. One of the major problems associated with such template-directed methods is the difficulty in achieving single-crystalline nanowires in large quantities.

Among the physical methods, evaporation, liquid-phase injection into channels of alumina templates [10.32, 34], as well as breaking up of elongated molten filaments under shear force [10.51, 52] have been utilized to obtain nanostructures of bismuth.

Chemical growth of bismuth nanocrystals was demonstrated by a set of various chemical processes including hydrothermal reactions [10.35, 65], synthesis in reverse micelles [10.66], decomposition/reduction of organometallic precursors and inorganic bismuth salts [10.35, 65, 67, 70–72, 76], and PVP- and/or polyol-mediated syntheses [10.50, 51, 68]. Polyol-mediated methods are of great importance as they allow large-scale synthesis, and most importantly the shape and size of the particles are easy to control by adjusting the ratio of reactants [10.68]; For instance, *Wang* and coworkers [10.73] (Fig. 10.2d) showed that, depending on the Bi/PVP ratio, nanocubes, triangular nanoplates (Fig. 10.2c), and nanospheres of bismuth could be obtained. By adding a trace amount of Fe^{3+}, nanobelts may also be produced.

Sn and In nanostructures are mostly synthesized in a similar fashion to Pb and Bi (i. e., physical vapor deposition and chemical reduction in templates or in solution) [10.43, 47, 77–79]; however, due to the very low standard reduction potential of In ($E^\circ = -0.34\,\text{V}$), stronger reduction conditions are usually needed than are applied for the other metals [10.43, 77–79].

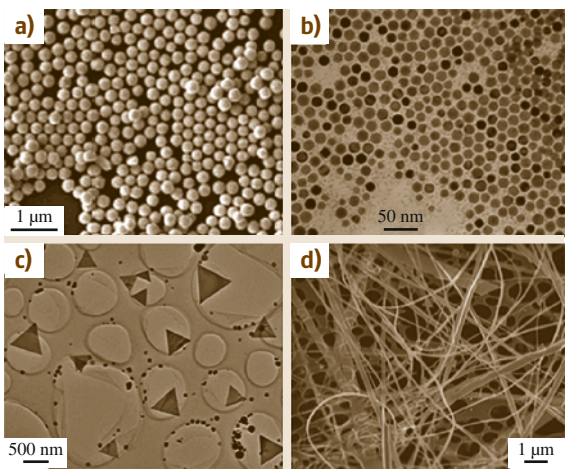

Fig. 10.2 **(a)** SEM image of Bi spherical colloids prepared by the top-down method. (After [10.51], 2012 ACS) **(b)** TEM image of Bi nanoparticles. (After [10.70], 2012, RSC) **(c,d)** TEM and SEM images of Bi triangular nanoplates and nanobelts. (After [10.73])

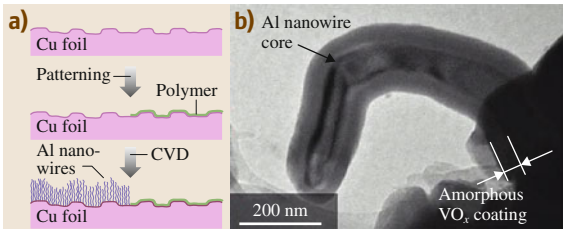

Fig. 10.3 (a) Schematic of CVD growth of Al nanowires. (b) TEM image of VO_x-coated Al nanowire. (After [10.80])

10.1.2 Aluminum

Owing to its wide variety of beneficial properties – such as low density, high strength-to-weight ratio, ductility, electrical conductivity, and corrosion resistance – bulk-phase metallic aluminum is widely used in the packaging, transport, and construction industries, in household appliances, in electronic devices, etc. It is worth pointing out that Al is one of the most abundant elements in the Earth's crust; however, it is almost always found combined with other elements due to its high reactivity. Because of the low standard reduction potential ($E^\circ = -1.66\,\mathrm{V}$), aluminum ions can be reduced almost only with alkali metals. In practice, electrolysis of a melt of Na_3AlF_3-Al_2O_3-CaF_2 (and alternatively other additives such as AlF_3, MgF_2, and KF) is applied for bulk production [10.81]. To date, two main types of methods have been developed for low-temperature electrochemical deposition of Al from nonaqueous solutions. For the first procedure, which was demonstrated in the 1950s [10.82], $AlCl_3$ together with $LiAlH_4$ or LiH is dissolved either in tetrahydrofuran or diethylether. In recent electrochemical deposition techniques, various ionic liquids [10.83–85] are used as solvents for aluminum chloride.

Aluminum nanostructures have been researched and used for several decades in optical coatings and in electrically conductive wiring in micro- and nanoelectronics, since Al thin films are quite easy to produce by thermal evaporation [10.86, 87] and sputtering of the pure metal or by chemical vapor deposition, e.g., from Al-alkyl precursors [10.88–90]. Nanosized patterns of thin Al films are routinely obtained by e-beam lithography [10.91, 92]. A further advantage of using aluminum is the thin, self-limiting native oxide layer, which grows rapidly on exposure of the surface to ambient air. This oxide may be directly used as electrically insulating passivation, or it can be etched easily if not needed. Apart from electrical and optical devices, Al nanoparticles (NPs) have also attracted interest as a future fuel or propellant material owing to the energetic bonds that form on oxidation of Al with oxygen or halogens [10.93, 94].

Various methods to produce aluminum nanostructures have been reported lately. *Mahendiran* and coworkers [10.95] demonstrated synthesis of NPs of ca. 25 nm diameter from a solution of $AlCl_3$ and $LiAlH_4$ in THF using a combined electro- and sonochemical route. *Foley* et al. reported a chemical route, in which triethylamine alane in heptane solution is decomposed at 70 °C in the presence of Ti-isopropoxide, yielding NPs with size from 50 to 500 nm [10.96]. Pulsed laser ablation of Al targets under ethanol or in vacuum – as a rather generic route to prepare various metal nanoparticles – has also been utilized to form Al NPs [10.97–99].

Template-directed techniques offer a plausible way to grow Al nanowires (NWs) too. Electrodeposition from ionic-liquid-based electrolytes [10.100, 101] and injection molding of molten Al metal [10.102] in porous templates have been reported. Aluminum nanowires can be synthesized, in a similar fashion as Zn or Sn, by employing physical vapor deposition (PVD) techniques based on vapor–solid (VS) growth mechanism [10.80, 103]. *Benson* and coworkers decomposed $H_3AlN(CH_3)_3$ precursor at temperatures of 125–300 °C to produce Al nanowires of 45–85 nm diameter on Ni, Cu, and steel surfaces and then used them as a large-specific-surface electrode material for supercapacitor application (Fig. 10.3) [10.80].

10.2 Transition Metals

The elements of the d-block are usually referred to as transition metals and have an incomplete outer d-shell of electrons. In a strict sense, Zn with its electron configuration $[Ar]3d^{10}4s^2$ is not a member of this group, and actually shows quite similar chemical properties to alkali-earth elements. Since most textbooks treat the elements of the Zn group together with the transition metals, here we also discuss it along with copper and some of the refractory metals [10.24, 25, 104]. Titanium, tungsten, molybdenum, and tantalum as hard, mechanically and thermally durable materials are listed after each other in this section. Not only their physical but

also their chemical properties – stemming from their relatively low standard reduction potentials – tie these elements together.

10.2.1 Titanium

Physical vapor deposition methods are among the plausible routes to form nanosized structures of titanium. Evaporated thin films and e-beam lithography-defined patterns represent the mainstream of fabrication, and are used in generating catalyst nanoparticles, thin coatings, as well as electrical components.

Electron-beam-deposited thin (< 1 nm) titanium films have been applied as a solid precursor on a Si surface for titanium silicide nanoparticle formation. When annealing the film in H_2 at 670–900 °C, the metal diffuses into the substrate and forms a silicide phase, which is catalytically active for subsequent chemical vapor deposition (CVD) of Si nanowires [10.106].

Lehtinen and coworkers fabricated Ti nanowires (tens of micrometers long, less than 50 nm in diameter) on a Si surface using e-beam lithography followed by evaporation in ultrahigh-vacuum conditions. Low-energy ion milling was applied to decrease the diameter of the nanowires, allowing size-dependent analysis of electrical transport behavior. Experiments carried out below 1 K showed that the critical temperature for superconductivity is reduced and that broadening of the transition temperature range occurs with decreasing wire diameter. This latter effect is due to quantum fluctuations of the order parameter, which may be utilized to construct new quantum devices such as qubits and standards of electric current [10.107, 108].

Titanium is known to form strong bonds with a number of different types of solid surfaces, and thus Ti (and also W and Ta) is frequently used as an adhesion-promoter sublayer for thin films of other metals (such as Au, Pt, Cu, and Ni) to be deposited on plastics or metal oxides/nitrides [10.109]. While most of the metals directly adhere to Ti, the reason for good sticking to oxides (and some polymers) is the −OH-terminated Ti surface, which may easily form when the surface is exposed to ambient air or to traces of oxygen and water vapor in the vacuum chamber. The interaction between the hydroxyl groups of a Ti surface and, e.g., the hydroxyl, carboxyl, and amine groups of the other surface can result in H-bonding or eventually in covalent Ti-O-Me (where Me is a metal) bonds if a condensation reaction takes place, similar to those exploited in nanotransfer printing [10.110]. Carbon also seems to have a reasonably strong interaction with titanium, as

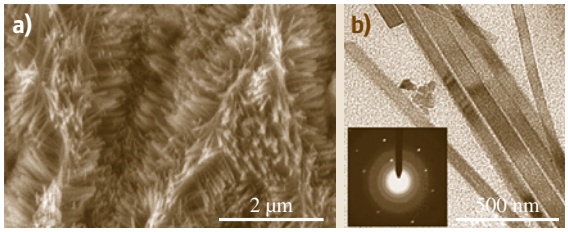

Fig. 10.4 (**a**) SEM and (**b**) TEM images of Ti nanowires synthesized on a Ti plate in 5% HCl solution at 180 °C. *Inset* shows a selected-area electron diffraction pattern. (After [10.105])

concluded by Zhang and Dai after studying e-beam-evaporated Ti films deposited on single-walled carbon nanotubes (SWCNT). Titanium films form thin continuous coatings, in contrast to other metals (such as Au, Pd, Fe, and Al), which tend to agglomerate to particles. The as-made Ti coating may be used as a metal nanotube with a coaxial carbon nanotube (CNT) interior, or alternatively can be applied as a buffer layer or adhesion promoter for other metals, thus enabling synthesis of multilayer structures having single-walled carbon nanotubes in their core, Ti in the mid-layer, and a tubular metal coating layer (Au, Pd, Fe, and Al) outside [10.111].

While pulsed laser ablation (PLA) of a Ti target in vacuum has been demonstrated as a potential tool for generating nanoparticles of Ti [10.112, 113], somehow PLA has not become a practical production method for metallic Ti NPs during the past years. Instead, TiO_2 nanoparticles have been synthesized by ablating a metal target submerged in water [10.114–116].

Chemical synthesis of Ti has also been demonstrated by a variety of methods. Though it was found impossible to reduce Ti^{4+} to Ti with $NaBH_4$ in ionic liquids [10.117], chemical vapor deposition from a $TiCl_4$ precursor at 640–670 °C followed by annealing in H_2 at 920 °C was sufficient to produce Ti-rich nanosized islands on Si wafers and to form $TiSi_2$ catalyst particles for subsequent Si nanowire synthesis [10.118]. *Corrias* and coworkers applied potassium intercalated multi-walled carbon nanotubes (MWCNTs) as templates with reducing behavior to generate α-Ti (hexagonal close-packed, hcp) nanoparticles of 2 nm size on the surfaces of CNTs from Ti isopropoxide [10.119].

A facile route to produce Ti nanowires on Ti plates was proposed by *Wu* and coworkers [10.105]. In their method, Ti surfaces were etched in dilute (5%) aqueous HCl solution at elevated temperature (150–200 °C) in an autoclave, resulting in the for-

mation of nanowire forests on the surface (Fig. 10.4). When decorated with Pt nanoparticles, the Ti nanowire-supported materials could be used as high specific surface area catalytic electrodes with low charge-transfer resistance ($85\,\Omega/cm^2$), e.g., for oxidation of methanol [10.105].

Another interesting route to produce Ti nanowires was proposed by *Huang* et al. [10.121]. They used electrochemical (anodic) etching of NiTi substrates in 20% H_2SO_4 and 80% methanol solution (at 18 V for 60 s), yielding single-crystal titanium nanowires along the ⟨110⟩ directions of the substrate.

While both chemical- and electrochemical etching techniques were suitable to form Ti nanostructures on Ti or Ti-containing surfaces, attempts to obtain metallic Ti on conductive surfaces by electrodeposition seemed to fail. In their work, *Endres* et al. showed that metallic titanium cannot be electrodeposited from titanium halides and isopropoxide when using ionic liquids (ILs) as solvents despite the wide electrochemical window offered by the solvents. They suppose that the underlying reason is the insolubility of partially reduced nonstoichiometric halide and oxide products in the ILs [10.122].

As synthesis of truly metallic Ti nanostructures is mainly limited to low-throughput methods, applications of such structures have not really spread into daily use in commercial devices. However, once large-scale production of Ti nanoparticles or nanowires and their packaging to prevent, e.g., their oxidation become possible, a series of novel and fascinating applications may be realized according to computational studies reported lately.

First-principles total-energy calculations revealed that Ti atoms adsorbed on the surface of SWCNTs are able to bond four H_2 molecules per Ti atom because of a unique hybridization of the Ti-d, H-σ*, and C-p orbitals. Though calculations for nanoparticles were not performed, the results suggest hydrogen storage and catalyst applications [10.3]. Molecular dynamics (MD) simulations showed that ultrathin ($d < 2$ nm) Ti NWs have helical structure with molecule-like electronic states for diameters below 1 nm and bulk-like behavior above that [10.5]. The melting temperature of similar ultrathin Ti NWs with multishell cylindrical structures was calculated (by MD simulations) to be lower than that of the bulk metal but higher than that of nanoparticles of similar size (i. e., less than 1.2 nm in diameter). The computed smooth heat capacity versus temperature curve and the sensitivity of bond length fluctuation to temperature suggest the coexistence of liquid and solid phases due to finite-size effects [10.4, 6]. Though bulk Ti is a paramagnetic material, deformed nanowires of Ti are predicted to show ferromagnetic ordering due to the polarization of the d-electron states [10.7, 8].

10.2.2 Tungsten

Large amounts of bulk-phase tungsten are used in hard materials such as tungsten carbide and in alloys that provide high mechanical strength and corrosion resistance. Owing to its good electrical conductivity and good wetting properties, tungsten is a component of under-metallization layers in integrated circuits (similar to titanium and molybdenum). Its high melting point and low vapor pressure at elevated temperatures allow high-temperature applications in vacuum tube filaments, heating elements, and incandescence lamps.

Interest in tungsten nanostructures has been growing steadily as they may find use in applications as pH-sensitive electrodes [10.123], atomic force microscopy probes [10.124], and field emitters [10.125, 126], and in components of nanoelectromechanical systems [10.127].

Metal nanoparticles can be obtained by reducing tungsten oxides at 500 °C in H_2 [10.128], in contrast to microparticles requiring 900 °C [10.129]. Nanoparticles of tungsten (with oxide shell) have also been prepared by reducing a metal complex by an organopolysilane oligomer at low temperature [10.130]. Further synthesis procedures include thermal decompo-

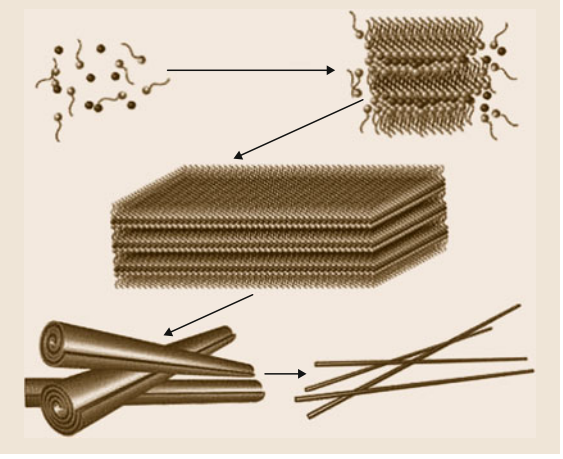

Fig. 10.5 Growth mechanism of tungsten nanowires by a vacuum pyrolysis carbothermal (VPC) process from a mesolamellar precursor. (After [10.120])

Fig. 10.6 Tungsten nanowires prepared by directional solidification and electrochemical processing of NiAl-W eutectic alloy. (After [10.140], courtesy of Wiley-VCH)

sition of $W(CO)_6$ [10.131, 132], sonoelectrochemical reduction from citrate complexes [10.133], e-beam-induced radiation damage of WO_3 [10.134], pulsed laser ablation of a W target in He atmosphere [10.135], ultraviolet (UV) laser-assisted chemical vapor deposition from $WF_6/H_2/Ar$ [10.136], and e-beam-induced decomposition of $W(CO)_6$ [10.137, 138]. Besides nanoparticles, only a few reports have been published on synthesis of one-dimensional tungsten nanostructures [10.120, 139–141].

In a novel method, metallic tungsten nanowires with diameters of 20–80 nm and lengths of several micrometers have been obtained in large quantities [10.120] by *Li* and coworkers. First, mesolamellar tungsten oxide-surfactant precursor (WO-L) was generated under mild hydrothermal conditions. Then, a vacuum pyrolysis/carbothermal (VPC) process was applied to remove the surfactant species from the lamellar inorganic-surfactant precursor. The authors proposed a new mechanism (Fig. 10.5) for the nanowire formation including four steps:

1. Evolution of cetyltrimethylammonium (CTA)–WO_4 ion pairs
2. Formation of highly ordered lamellar assemblies
3. Development of scrolls by rolling up of lamellar sheets owing to vacuum heating
4. Reduction of tungstate by pyrolytic carbon.

High-aspect-ratio single-crystalline NWs with a thin oxide layer were successfully synthesized by directional solidification and electrochemical processing of NiAl-W eutectic alloy (Fig. 10.6) [10.140] and by rapid thermal annealing of W films [10.126]. Catalytic synthesis based on a vapor–solid–solid (VSS) mechanism route was reported by Wang and coworkers. Tungsten powder mixed and then annealed together with $NiNO_3$ was used to prepare WO_3 and $NiWO_4$, which in turn was reduced with H_2 [10.142] to obtain W nanowires as the product with Ni nanoparticles at the tip of the wires.

10.2.3 Molybdenum

Bulk molybdenum is primarily utilized in metallurgy to prepare alloys with advanced wear- and corrosion-resistance behavior. When going to the nanoscale, direct applications of Mo are very rare and limited to catalysis mainly. Though nanoparticles or clusters of this metal are relatively easy to synthesize by both chemical [10.9, 143–148] and physical [10.149–151] methods, its practical/industrial relevance – other than in catalysis – seems to be negligible compared with molybdenum oxides and sulfides, and is mainly the focus of academic research today [10.10–13].

However, molybdenum sulfides and oxides are widely studied and used, e.g., in tribology (wear and friction of surfaces) [10.152, 153], in catalysis [10.154–161], and in catalytic electrodes for supercapacitors and fuel cells [10.162–165], as well as holding promise for use in novel electrical components [10.166–168]. So far, the petrol industry has been the major user of MoS_2 catalyst nanoparticles (and their different modified derivatives) on alumina support for hydrodesulfurization (HDS) of hydrocarbons [10.154–157]. Apart from HDS, sulfides are also considered to be useful in catalyzing methanation [10.158] and in H_2 generation reactions [10.159, 160].

10.2.4 Tantalum

While nanostructures of carbides, oxides, nitrides, oxynitrides, and sulfides of tantalum are routinely synthesized by, e.g., vapor–solid reaction, chemical vapor deposition, laser ablation, surface-assisted chemical vapor transport, anodization, and sputtering, and used in superconductor, photocatalyst, and other applications, research on metallic Ta nanoparticles is rather sparse [10.169–179]. The reason is similar to that of other transition metals: it is difficult to reduce from its oxidized state, and once reduced, it is prone to oxidation under common environmental conditions. There are, however, some interesting methods to produce and utilize Ta nanostructures.

Mativetsky and coworkers have grown nanoparticles (and self-aligned chains of those along surface

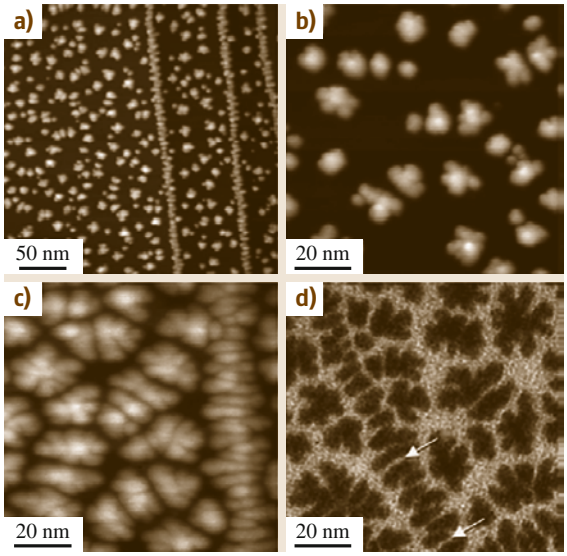

Fig. 10.7a–d Tantalum nanoparticles formed on KBr 001 surface after e-beam deposition of **(a,b)** 0.6 and **(c,d)** 1.8 molecular layers. Images in panels **(a–c)** were acquired using non-contact-mode atomic force microscopy, while the image in panel **(d)** was taken by transmission electron microscopy. *Arrows* indicate gaps between adjacent nanoparticles nucleated at a step. (After [10.180])

steps) on single-crystal KBr by e-beam deposition (Fig. 10.7). Despite the cubic lattice of the substrate, the Ta particles form as separate islands with fractal-like shape, suggesting poor interaction between the substrate and the nanoparticles [10.180].

Nanoparticles of Ta were shown to form in a H_2/Ar arc plasma when applying bulk Ta as both anode and cathode material. Because of the high temperature, the electrodes start to melt and evaporate, leading to a vapor of metal atoms and clusters, which thermalize and coalesce through collisions, thus forming nanoparticles [10.182].

Besides the aforementioned physical methods, chemical routes may also be possible under strongly reducing conditions. Metal-graphite multilayer (MGM) structures may be obtained by intercalating metal chlorides for instance with natural or highly oriented pyrolytic graphite (NG or HOPG, respectively) followed by chemical reduction of the chloride in H_2 flow at elevated temperatures [10.183, 184]. Using a two-step procedure reported by Walter et al., first, anhydrous $TaCl_5$ is mixed with HOPG and stored in Cl_2 atmosphere at 400 °C for 4 days, then exposed to H_2 gas at 1000 °C for 1 week to prepare Ta nanoparticles intercalated with the graphene layers in graphite. The as-obtained structures behave as superconductors similar to tantalum carbide. As suggested by *Suzuki* and coworkers, the Ta nanoparticles act as localized spins, which can couple with the adjacent layers separated by the graphitic layers [10.184].

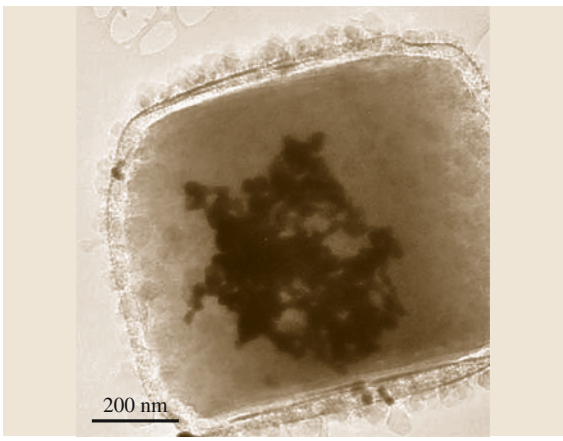

Fig. 10.8 TEM image of salt-encapsulated Ta nanoparticles synthesized by the sodium/halide gas-phase (flame) combustion process. (After [10.181])

Axelbaum and colleagues developed and patented a technology capable of producing large volumes of nanopowders of metals as well as their composites by reacting sodium vapor with gas-phase metal chlorides in a flame [10.181, 185] (Fig. 10.8). At high temperatures, Na vapor reduces metal (such as Ta, Ti, Al, Nb, Si, W, or Fe) chlorides (or other halides) and produces metal nanoparticles. By controlling the temperature and heat losses in the reactor, condensation of the byproduct NaCl vapor on the metal nanoparticles can be regulated. Increased temperature favors sublimation of the salt and consequently the formation of larger metal nanoparticle cores, while lower temperatures result in condensation of the salt vapor on the core. The as-formed shell acts as a barrier coating, protecting the metal core from moisture and air. The salt encapsulation can be removed, for instance, by vacuum sublimation, thus releasing the Ta nanoparticles for their end use.

10.2.5 Zinc

Zinc is an industrially important metal applied in large quantities in batteries, anticorrosion coatings, and various structural alloys today. Most of the studies related to elemental zinc are focused on the generation of zinc

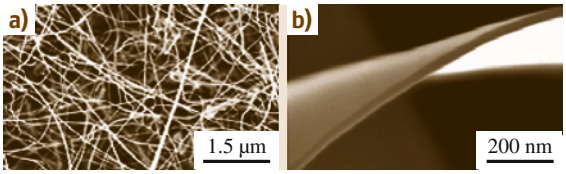

Fig. 10.9 Low- **(a)** and high-magnification **(b)** SEM images of Zn nanobelts. (After [10.190])

chalcogenide nanostructures due to their semiconducting and piezo- and pyroelectric properties, which find applications in pigments and (photo)catalytic processes, and thus are widely studied in the contemporary literature [10.186–189].

Vapor–solid (VS) growth of Zn nanowires has been reported by several groups. In this method, a vapor of Zn is generated first under protective gas, by either evaporating pure metal [10.191] or decomposing organic zinc compounds [10.192], or by reacting ZnO or ZnS with carbon, ammonia, H_2, etc. at elevated temperature [10.190, 193, 194]. When the vapor of Zn enters a colder zone of the reactor (typically a two-zone furnace is employed), condensation of the vapor starts and Zn nanowires are observed to grow. Since the process is not catalyzed by any separate nanoparticle or seed, it is referred to as VS growth [10.191]. To produce nanoparticles, PLA has been applied [10.195, 196]. Most of these studies, however, agree that Zn nanostructures are covered by a thin layer of ZnO [10.191, 193, 195] (Fig. 10.9a,b).

Solution-phase synthesis of Zn nanomaterials has not been widely explored, since the procedure has to be conducted under inert gas protection to avoid oxidation. Electrochemical deposition as one of the major synthesis tools for metallic zinc has been successfully utilized to prepare both single- and polycrystalline nanowires with diameter of 40–100 nm in porous AAO and PTCE membranes [10.197].

10.2.6 Copper

In everyday life, copper is used for several kinds of applications and devices. One major advantage of copper, compared with other metals, is its excellent electrical conductivity, which is greater than that of any other metal apart from silver. Most copper is used in electrical wires for motors, transformers, cars, integrated circuits, etc. to transfer electrical energy in an efficient manner with minimal environmental impact. Copper is also widely used in heat exchangers and heat sinks due to its high thermal conductivity. Other attractive properties of this metal are its durability, corrosion resistance, and antimicrobial effect, which enable a vast number of applications in the construction industry as a structural and alloying material, and as a functional surface coating.

Most probably, catalysis and electronics are the two main fields that could greatly benefit from the availability of copper nanostructures. In the last decades, copper nanostructures with various morphologies and oxidation states have been widely studied for applications in heterogeneous catalysis [10.198–200]. Furthermore, the surface chemistry on Cu has also been elaborated in detail by *Somorjai* et al. [10.201]. Copper, particularly in nanoparticle form [10.202], has found use as a catalyst in water–gas shift reactions [10.200,203,204], methanol synthesis [10.205–207], aryl homocoupling [10.208], growth of Si nanowires by chemical vapor deposition (CVD) [10.209], etc.

One of the very first methods for preparation of Cu nanowires (which were encapsulated in carbon nanotubes) was demonstrated by *Setlur* et al. in a hydrogen arc between a graphite cathode and a graphite–copper anode [10.210]. Evaporation and subsequent condensation of Cu, forming nanorods and nanowires at 10^{-4} Pa pressure in a transmission electron microscope (TEM) column, was reported by *Liu* and *Bando* [10.211]. Though several other physical methods such as laser ablation [10.212, 213], pulsed wire discharge [10.214], and evaporation [10.215] exist, because of their limited production volume and associated price, the aforementioned physical methods are surpassed by the chemical ones, since a number of different reaction routes enable the production of nanoparticles of different sizes and shapes, even in a simple beaker under mild conditions [10.216–228]. The key to obtaining various crystal shapes is the presence of surface-capping agents (to selectively adsorb onto and block specific crystal planes) [10.17, 229] or addition of ionic impurities [10.69, 225].

Hexagonal nanoplates of copper have been prepared by reduction of $Cu(CH_3CO_2)_2$ with hydrazine hydrate in acetonitrile [10.226]. Nanoparticles of cubic, tetrahedral, and rod shapes with size ranging from 5 to 25 nm were obtained by reduction of copper acetylacetonate with 1,2-hexadecanethiol in octyl ether in the presence of oleyl amine and oleic acid serving as capping molecules [10.227]. Cu nanowires with diameter of ca. 85 nm were prepared by a complex-surfactant-assisted hydrothermal route from Cu(II)–glycerol complexes reduced by phosphite in the presence of sodium dodecyl benzenesulfonate (SDBS) [10.221]. Recently,

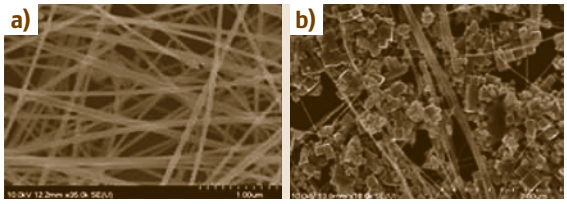

Fig. 10.10 (**a**) SEM image of Cu nanowires prepared by a hydrothermal process in the presence of hexadecylamine (HDA). (**b**) SEM image of Cu nanocubes. (After [10.220])

Fig. 10.11 CuPd bimetallic nanotubes prepared by galvanic exchange reaction on Cu nanowires. (After [10.232])

we reported a very rapid route to ultralong copper nanowires (Fig. 10.10a) and nanocubes (Fig. 10.10b) on a large scale with HDA as capping agent [10.220]. In a typical synthesis, $CuCl_2$ and glucose were dissolved in water, followed by addition of hexadecylamine (HDA). After stirring for several hours, the light-blue solution was placed in an autoclave that was heated to 120 °C. In a recent study, this method was slightly modified by *Jin* and coworkers to produce single-crystal Cu nanowires [10.230]. In a similar hydrothermal route, polycrystalline and single-crystalline Cu nanowires were generated in the presence of octadecylamine [10.231]. Though copper has a positive standard electrode potential ($E^\circ = 0.34$ V) it is still rather easy to oxidize its surface, or even the entire volume of the material if it is nanostructured. For instance, exposing Cu nanowires to solvated cations of nobel metals (Pt^{2+} or Pd^{2+}) can initiate galvanic replacement reactions, in which the nanowires undergo oxidation and dissolution while the precious metal is depositing on the surface of copper thus forming nanotubes of CuPt or CuPd alloys [10.232] (Fig. 10.11).

It is worth mentioning that Cu nanostructures are prone to oxidation. Even trace amounts of oxygen dissolved in the solution of reactants can cause partial oxidation, causing sometimes controversial results, thus it still remains a great challenge to synthesize pure copper particles by solution-phase methods [10.69, 233–235]. One way to protect Cu seeds from oxidation during production is to apply a N_2 atmosphere and to purge the reaction solution with inert gases.

10.3 Concluding Remarks

In this chapter, we have provided an overview on nanostructures of metals excluding ferromagnetic and precious ones, which are described in Chap. 9. As most of the metals belong to this category, we organized them based on the following criteria:

1. Reasonable chemical stability under ordinary conditions
2. Abundance of raw materials
3. Industrial importance in bulk form.

As it turns out from the literature review, this particular field of materials science has not yet been fully explored. Some potential applications of the metal nanostructures are discussed in the cited literature. However, despite numerous reports on laboratory-scale synthesis, controlled bulk production and utilization of such nanostructures are still in the early stage of technical development and should be improved. Since the majority of these elements are prone to oxidation, difficulties related to chemical stability need to be studied and should be solved by surface engineering; otherwise nanostructures made of compounds of these metals are expected as a result. Besides the existing knowledge, further peculiarities of these materials at the nanoscale remain to be revealed to enable their wide use in novel technologies and devices.

References

10.1 A.S. Edelstein, R.C. Cammarata: *Nanomaterials: Synthesis, Properties and Applications* (Institute of Physics, Bristol 2002)

10.2 G. Schmid: *Nanoparticles: From Theory to Application* (Wiley-VCH, Weinheim 2011)

10.3 T. Yildirim, S. Ciraci: Titanium-decorated carbon nanotubes as a potential high-capacity hydrogen storage medium, Phys. Rev. Lett. **94**, 175501 (2005)

10.4 B. Wang, G. Wang, X. Chen, J. Zhao: Melting behavior of ultrathin titanium nanowires, Phys. Rev. B **67**, 193403 (2003)

10.5 B. Wang, S. Yin, G. Wang, J. Zhao: Structures and electronic properties of ultrathin titanium nanowires, J. Phys. Condens. Matter **13**, L403 (2001)

10.6 Y. Imry, D.J. Scalapino: Pseudo - first - order phase transitions in one dimension, Phys. Rev. A **9**, 1672–1675 (1974)

10.7 Z. Zhu, J. Gu, Y. Jia: Emergence of magnetism in titanium nanowires, J. Phys. Condens. Matter **387**, 190–193 (2007)

10.8 H.R. Hajiyani, M. Jafari: Magneto optical properties of β [110] and ω [100] titanium nanowires, J. Magn. Magn. Mater. **324**, 418–423 (2012)

10.9 H.K. Kim, S.H. Huh, J.W. Park, J.W. Jeong, G.H. Lee: The cluster size dependence of thermal stabilities of both molybdenum and tungsten nanoclusters, Chem. Phys. Lett. **354**, 165–172 (2002)

10.10 Y. Shibuta, T. Suzuki: Phase transition in substrate-supported molybdenum nanoparticles: A molecular dynamics study, Phys. Chem. Chem. Phys. **12**, 731–739 (2010)

10.11 Y. Shibuta, T. Suzuki: A molecular dynamics study of the phase transition in bcc metal nanoparticles, J. Chem. Phys. **129**, 144102 (2008)

10.12 W. Zhang, X. Ran, H. Zhao, L. Wang: The nonmetallicity of molybdenum clusters, J. Chem. Phys. **121**, 7717–7724 (2004)

10.13 W.H. Qi: Comment on: The cluster size dependence of thermal stabilities of both molybdenum and tungsten nanoclusters, Chem. Phys. Lett. **402**, 279–281 (2005)

10.14 C.G. Granqvist, R.A. Buhrman: Ultrafine metal particles, J. Appl. Phys. **47**, 2200–2219 (1976)

10.15 K. Sattler, J. Muhlbach, E. Recknagel: Generation of metal clusters containing from 2 to 500 atoms, Phys. Rev. Lett. **45**, 821–824 (1980)

10.16 C.W. Won, H.H. Nersisyan, H.I. Won, J.H. Lee: Refractory metal nanopowders: Synthesis and characterization, Curr. Opin. Solid State Mater. Sci. **14**, 53–68 (2010)

10.17 M. Mohl: Egydimenziós fém nanoszerkezetek előállítása és vizsgálata/Preparation and Characterization of One-Dimensional Nanostructures, Dissertation (University of Szeged, Hungary 2011)

10.18 R.W. Murray: Nanoelectrochemistry: Metal nanoparticles, nanoelectrodes, and nanopores, Chem. Rev. **108**, 2688–2720 (2008)

10.19 B.R. Cuenya: Synthesis and catalytic properties of metal nanoparticles: Size, shape, support, composition, and oxidation state effects, Thin Solid Films **518**, 3127–3150 (2010)

10.20 C.N.R. Rao, G.U. Kulkarni, P.J. Thomas, P.P. Edwards: Metal nanoparticles and their assemblies, Chem. Soc. Rev. **29**, 27–35 (2000)

10.21 A. Tavakoli, M. Sohrabi, A. Kargari: A review of methods for synthesis of nanostructured metals with emphasis on iron compounds, Chem. Pap. **61**, 151–170 (2007)

10.22 K. Watanabe, D. Menzel, N. Nilius, H. Freund: Photochemistry on metal nanoparticles, Chem. Rev. **106**, 4301–4320 (2006)

10.23 H.M. Chen, R. Liu: Architecture of metallic nanostructures: Synthesis strategy and specific applications, J. Phys. Chem. C **115**, 3513–3527 (2011)

10.24 D.R. Lide: *Handbook of Chemistry and Physics*, 72nd edn. (CRC, Boca Raton 1991–1992)

10.25 P. Atkins, T. Overton, J. Rourke, M. Weller, F. Armstrong: *Shriver and Atkins Inorganic Chemistry* (Oxford University Press, New York 2006)

10.26 MatWeb: Material Property Data (MatWeb LLC, Blacksburg 2012) available at http://www.matweb.com/index.aspx

10.27 J. Wang, Y. Sun, M. Tian, B. Liu, M. Singh, M.H.W. Chan: Superconductivity in single crystalline Pb nanowires contacted by normal metal electrodes, Phys. Rev. B **86**, 035439 (2012)

10.28 J. Wang, X. Ma, S. Ji, Y. Qi, Y. Fu, A. Jin, L. Lu, C. Gu, X. Xie, M. Tian, J. Jia, Q. Xue: Magnetoresistance oscillations of ultrathin Pb bridges, Nano Res. **2**, 671–677 (2009)

10.29 V.D. Das, N. Soundararajan: Size and temperature effects on the Seebeck coefficient of thin bismuth films, Phys. Rev. B **35**, 5990–5996 (1987)

10.30 Y. Ishikawa, Y. Hasegawa, H. Morita, A. Kurokouchi, K. Wada, T. Komine, H. Nakamura: Resistivity and Seebeck coefficient measurements of a bismuth microwire array, Phys. Condens. Matter **368**, 163–167 (2005)

10.31 V. Kamaev, V. Kozhevnikov, Z.V. Vardeny, P.B. Landon, A.A. Zakhidov: Optical studies of metallodielectric photonic crystals: Bismuth and gallium infiltrated opals, J. Appl. Phys. **95**, 2947–2951 (2004)

10.32 Z. Zhang, D. Gekhtman, M.S. Dresselhaus, J.Y. Ying: Processing and characterization of single-crystalline ultrafine bismuth nanowires, Chem. Mater. **11**, 1659–1665 (1999)

10.33 M. Tian, J. Wang, Q. Zhang, N. Kumar, T.E. Mallouk, M.H.W. Chan: Superconductivity and quantum os-

cillations in crystalline Bi nanowire, Nano Lett. **9**, 3196–3202 (2009)
10.34 Z. Zhang, J.Y. Ying, M.S. Dresselhaus: Bismuth quantum-wire arrays fabricated by a vacuum melting and pressure injection process, J. Mater. Res. **13**, 1745 (1998)
10.35 Y. Gao, H. Niu, C. Zeng, Q. Chen: Preparation and characterization of single-crystalline bismuth nanowires by a low-temperature solvothermal process, Chem. Phys. Lett. **367**, 141–144 (2003)
10.36 D. Gekhtman, Z.B. Zhang, D. Adderton, M.S. Dresselhaus, G. Dresselhaus: Electrostatic force spectroscopy and imaging of Bi wires: Spatially resolved quantum confinement, Phys. Rev. Lett. **82**, 3887–3890 (1999)
10.37 Z. Zhang, X. Sun, M.S. Dresselhaus, J.Y. Ying, J. Heremans: Electronic transport properties of single-crystal bismuth nanowire arrays, Phys. Rev. B **61**, 4850–4861 (2000)
10.38 S.H. Choi, K.L. Wang, M.S. Leung, G.W. Stupian, N. Presser, B.A. Morgan, R.E. Robertson, M. Abraham, E.E. King, M.B. Tueling, S.W. Chung, J.R. Heath, S.L. Cho, J.B. Ketterson: Fabrication of bismuth nanowires with a silver nanocrystal shadowmask, J. Vac. Sci. Technol. A **18**, 1326–1328 (2000)
10.39 M.R. Black, G. Dresselhaus, M.S. Dresselhaus: Nanowires. In: *Springer Handbook of Nanotechnology*, ed. by B. Bhushan (Springer, Berlin, Heidelberg 2004) pp. 99–138, http://www.springerlink.com/Content/g52qg1542050x561/
10.40 A.A. Shanenko, M.D. Croitoru, M. Zgirski, F.M. Peeters, K. Arutyunov: Size-dependent enhancement of superconductivity in Al and Sn nanowires: Shape-resonance effect, Phys. Rev. B **74**, 052502 (2006)
10.41 S. Michotte, S. Matefi-Tempfli, L. Piraux: Current–voltage characteristics of Pb and Sn granular superconducting nanowires, Appl. Phys. Lett. **82**, 4119–4121 (2003)
10.42 M. Tian, J. Wang, J.S. Kurtz, Y. Liu, M.H.W. Chan, T.S. Mayer, T.E. Mallouk: Dissipation in quasi-one-dimensional superconducting single-crystal Sn nanowires, Phys. Rev. B **71**, 104521 (2005)
10.43 N.H. Chou, X. Ke, P. Schiffer, R.E. Schaak: Room-temperature chemical synthesis of shape-controlled indium nanoparticles, J. Am. Chem. Soc. **130**, 8140–8141 (2008)
10.44 Y. Hsu, S. Lu, Y. Lin: Nanostructures of Sn and their enhanced, shape-dependent superconducting properties, Small **2**, 268–273 (2006)
10.45 M. Amagai: A study of nanoparticles in Sn-Ag based lead free solders, Microelectron. Reliab. **48**, 1–16 (2008)
10.46 C.L. Monica, G.J. Siri, G.F. Santori, O.A. Ferretti, M.M. Ramirez-Corredores: Surface characterization of Li-modified platinum/tin catalysts for isobutane dehydrogenation, Langmuir **16**, 5639–5643 (2000)
10.47 M. Noh, Y. Kim, M.G. Kim, H. Lee, H. Kim, Y. Kwon, Y. Lee, J. Cho: Monomer-capped tin metal nanoparticles for anode materials in lithium secondary batteries, Chem. Mater. **17**, 3320–3324 (2005)
10.48 N.H. Chou, R.E. Schaak: Shape-controlled conversion of β-Sn nanocrystals into intermetallic M-Sn (M=Fe, Co, Ni, Pd) nanocrystals, J. Am. Chem. Soc. **129**, 7339–7345 (2007)
10.49 Y. Wang, L. Cai, Y. Xia: Monodisperse spherical colloids of Pb and their use as chemical templates to produce hollow particles, Adv. Mater. **17**, 473–477 (2005)
10.50 Y. Wang, M. Ibisate, Z.Y. Li, Y. Xia: Metallodielectric photonic crystals assembled from monodisperse spherical colloids of bismuth and lead, Adv. Mater. **18**, 471–476 (2006)
10.51 Y. Wang, Y. Xia: Bottom-up and top-down approaches to the synthesis of monodispersed spherical colloids of low melting-point metals, Nano Lett. **4**, 2047–2050 (2004)
10.52 U. Jeong, Y. Wang, M. Ibisate, Y. Xia: Some new developments in the synthesis, functionalization, and utilization of monodisperse colloidal spheres, Adv. Funct. Mater. **15**, 1907–1921 (2005)
10.53 Y. Zhao, Z. Zhang, H. Dang: Fabrication and tribological properties of Pb nanoparticles, J. Nanopart. Res. **6**, 47–51 (2004)
10.54 Y. Wang, T. Herricks, Y. Xia: Single crystalline nanowires of lead can be synthesized through thermal decomposition of lead acetate in ethylene glycol, Nano Lett. **3**, 1163–1166 (2003)
10.55 X. Lin, H. Claus, U. Welp, I.S. Beloborodov, W. Kwok, G.W. Crabtree, H.M. Jaeger: Growth and properties of superconducting anisotropic lead nanoprisms, J. Phys. Chem. C **111**, 3548–3550 (2007)
10.56 J.D. Joannopoulos, J.N. Winn, R.D. Meade: *Photonic Crystals* (Princeton Univ. Press, Princeton 1995)
10.57 W.H. Li, C.C. Yang, F.C. Tsao, K.C. Lee: Quantum size effects on the superconducting parameters of zero-dimensional Pb nanoparticles, Phys. Rev. B **68**, 184507 (2003)
10.58 Y. Wang, X. Jiang, T. Herricks, Y. Xia: Single crystalline nanowires of lead: Large-scale synthesis, mechanistic studies, and transport measurements, J. Phys. Chem. B **108**, 8631–8640 (2004)
10.59 T.J. Trentler, K.M. Hickman, S.C. Goel, A.M. Viano, P.C. Gibbons, W.E. Buhro: Solution-liquid-solid growth of crystalline III–V semiconductors: An analogy to vapor-liquid-solid growth, Science **270**, 1791–1794 (1995)
10.60 S. Dubois, A. Michel, J.P. Eymery, J.L. Duvail, L. Piraux: Fabrication and properties of arrays of superconducting nanowires, J. Mater. Res. **14**, 665–671 (1999)
10.61 Y.T. Pang, G.W. Meng, L.D. Zhang, Y. Qin, X.Y. Gao, A.W. Zhao, Q. Fang: Arrays of ordered Pb nanowires

and their optical properties for laminated polarizers, Adv. Funct. Mater. **12**, 719–722 (2002)
10.62 M. Jałochowski, E. Bauer: Growth of metallic nanowires on anisotropic Si substrates: Pb on vicinal Si(001), Si(755), Si(533), and Si(110), Surf. Sci. **480**, 109–117 (2001)
10.63 M. Jałochowski, E. Bauer: Self-assembled parallel mesoscopic Pb-wires on Au-modified Si(533) substrates, Prog. Surf. Sci. **67**, 79–97 (2001)
10.64 G. Yi, W. Schwarzacher: Single crystal superconductor nanowires by electrodeposition, Appl. Phys. Lett. **74**, 1746–1748 (1999)
10.65 J. Wang, Y. Li: Rational synthesis of metal nanotubes and nanowires from Lamellar structures, Adv. Mater. **15**, 445–447 (2003)
10.66 E.E. Foos, R.M. Stroud, A.D. Berry, A.W. Snow, J.P. Armistead: Synthesis of nanocrystalline bismuth in reverse micelles, J. Am. Chem. Soc. **122**, 7114–7115 (2000)
10.67 M. Gutierrez, A. Henglein: Nanometer-sized Bi particles in aqueous solution: Absorption spectrum and some chemical properties, J. Phys. Chem. **100**, 7656–7661 (1996)
10.68 J. Wang, X. Wang, Q. Peng, Y. Li: Synthesis and characterization of bismuth single-crystalline nanowires and nanospheres, Inorg. Chem. **43**, 7552–7556 (2004)
10.69 Y. Xia, Y. Xiong, B. Lim, S.E. Skrabalak: Shape-controlled synthesis of metal nanocrystals: Simple chemistry meets complex physics?, Angew. Chem. Int. Ed. **48**, 60–103 (2009)
10.70 J. Fang, K.L. Stokes, W.L. Zhou, W. Wang, J. Lin: Self-assembled bismuth nanocrystallites, Chem. Commun., 1872–1873 (2001)
10.71 J. Wang, G. Cao, Y. Li: Giant positive magnetoresistance in non-magnetic bismuth nanoparticles, Mater. Res. Bull. **38**, 1645–1651 (2003)
10.72 H. Yu, P.C. Gibbons, K.F. Kelton, W.E. Buhro: Heterogeneous seeded growth: A potentially general synthesis of monodisperse metallic nanoparticles, J. Am. Chem. Soc. **123**, 9198–9199 (2001)
10.73 W.Z. Wang, B. Poudel, Y. Ma, Z.F. Ren: Shape control of single crystalline bismuth nanostructures, J. Phys. Chem. B **110**, 25702–25706 (2006)
10.74 J. Heremans, C.M. Thrush, Y. Lin, S. Cronin, Z. Zhang, M.S. Dresselhaus, J.F. Mansfield: Bismuth nanowire arrays: Synthesis and galvanomagnetic properties, Phys. Rev. B **61**, 2921–2930 (2000)
10.75 K. Liu, C.L. Chien, P.C. Searson, K. Yu-Zhang: Structural and magneto-transport properties of electrodeposited bismuth nanowires, Appl. Phys. Lett. **73**, 1436–1438 (1998)
10.76 Y. Li, J. Wang, Z. Deng, Y. Wu, X. Sun, D. Yu, P. Yang: Bismuth nanotubes: A rational low-temperature synthetic route, J. Am. Chem. Soc. **123**, 9904–9905 (2001)
10.77 P.K. Khanna, K. Jun, K.B. Hong, J. Baeg, R.C. Chikate, B.K. Das: Colloidal synthesis of indium nanoparticles by sodium reduction method, Mater. Lett. **59**, 1032–1036 (2005)
10.78 K. Soulantica, A. Maisonnat, F. Senocq, M. Fromen, M. Casanove, B. Chaudret: Selective synthesis of novel In and In_3Sn nanowires by an organometallic route at room temperature, Angew. Chem. Int. Ed. **40**, 2983–2986 (2001)
10.79 K. Soulantica, A. Maisonnat, M. Fromen, M. Casanove, P. Lecante, B. Chaudret: Synthesis and self-assembly of monodisperse indium nanoparticles prepared from the organometallic precursor $[In(\eta^5\text{-}C_5H_5)]$, Angew. Chem. Int. Ed. **40**, 448–451 (2001)
10.80 J. Benson, S. Boukhalfa, A. Magasinski, A. Kvit, G. Yushin: Chemical vapor deposition of aluminum nanowires on metal substrates for electrical energy storage applications, ACS Nano **6**, 118–125 (2012)
10.81 L. Cassayre, P. Palau, P. Chamelot, L. Massot: Properties of low-temperature melting electrolytes for the aluminum electrolysis process: A review, J. Chem. Eng. Data **55**, 4549–4560 (2010)
10.82 D.E. Couch, A. Brenner: A hydride bath for the electrodeposition of aluminum, J. Electrochem. Soc. **99**, 234–244 (1952)
10.83 S. Zein El Abedin, E.M. Moustafa, R. Hempelmann, H. Natter, F. Endres: Electrodeposition of nano- and microcrystalline aluminium in three different air and water stable ionic liquids, Chem. Phys. Chem. **7**, 1535–1543 (2006)
10.84 N. Koura, H. Nagase, A. Sato, S. Kumakura, K. Takeuchi, K. Ui, T. Tsuda, C.K. Loong: Electroless plating of aluminum from a room-temperature ionic liquid electrolyte, J. Electrochem. Soc. **155**, D155–D157 (2008)
10.85 J. Chang, S. Chen, W. Tsai, M. Deng, I. Sun: Electrodeposition of aluminum on magnesium alloy in aluminum chloride ($AlCl_3$)-1-ethyl-3-methylimidazolium chloride (EMIC) ionic liquid and its corrosion behavior, Electrochem. Commun. **9**, 1602–1606 (2007)
10.86 F. Altomare, A.M. Chang, M.R. Melloch, Y. Hong, C.W. Tu: Ultranarrow AuPd and Al wires, Appl. Phys. Lett. **86**, 172501–172503 (2005)
10.87 F. Altomare, A.M. Chang, M.R. Melloch, Y. Hong, C.W. Tu: Evidence for macroscopic quantum tunneling of phase slips in long one-dimensional superconducting Al wires, Phys. Rev. Lett. **97**, 017001 (2006)
10.88 M. Zgirski, K. Riikonen, V. Touboltsev, K. Arutyunov: Size dependent breakdown of superconductivity in ultranarrow nanowires, Nano Lett. **5**, 1029–1033 (2005)
10.89 S. Franssila: *Introduction to Microfabrication* (John Wiley & Sons, West Sussex, UK 2004)
10.90 T.A. Fulton, G.J. Dolan: Observation of single-electron charging effects in small tunnel junctions, Phys. Rev. Lett. **59**, 109–112 (1987)

10.91 P. Santhanam, C.C. Chi, S.J. Wind, M.J. Brady, J.J. Bucchignano: Resistance anomaly near the superconducting transition temperature in short aluminum wires, Phys. Rev. Lett. **66**, 2254–2257 (1991)

10.92 H. Tamada, T. Doumuki, T. Yamaguchi, S. Matsumoto: Al wire-grid polarizer using the s-polarization resonance effect at the 0.8-μm-wavelength band, Opt. Lett. **22**, 419–421 (1997)

10.93 D.D. Dlott: Thinking big (and small) about energetic materials, Mater. Sci. Technol. **22**, 463–473 (2006)

10.94 M.A. Zamkov, R.W. Conner, D.D. Dlott: Ultrafast chemistry of nanoenergetic materials studied by time-resolved infrared spectroscopy: Aluminum nanoparticles in teflon, J. Phys. Chem. C **111**, 10278–10284 (2007)

10.95 C. Mahendiran, R. Ganesan, A. Gedanken: Sonoelectrochemical synthesis of metallic aluminum nanoparticles, Eur. J. Inorg. Chem. **2009**, 2050–2053 (2009)

10.96 T.J. Foley, C.E. Johnson, K.T. Higa: Inhibition of oxide formation on aluminum nanoparticles by transition metal coating, Chem. Mater. **17**, 4086–4091 (2005)

10.97 S. Eliezer, N. Eliaz, E. Grossman, D. Fisher, I. Gouzman, Z. Henis, S. Pecker, Y. Horovitz, M. Fraenkel, S. Maman, Y. Lereah: Synthesis of nanoparticles with femtosecond laser pulses, Phys. Rev. B **69**, 144119 (2004)

10.98 E. Stratakis, M. Barberoglou, C. Fotakis, G. Viau, C. Garcia, G.A. Shafeev: Generation of Al nanoparticles via ablation of bulk Al in liquids with short laser pulses, Opt. Express **17**, 12650–12659 (2009)

10.99 C.A. Crouse, E. Shin, P.T. Murray, J.E. Spowart: Solution assisted laser ablation synthesis of discrete aluminum nanoparticles, Mater. Lett. **64**, 271–274 (2010)

10.100 M. Singh, J. Wang, M. Tian, Q. Zhang, A. Pereira, N. Kumar, T.E. Mallouk, M.H.W. Chan: Synthesis and superconductivity of electrochemically grown single-crystal aluminum nanowires, Chem. Mater. **21**, 5557–5559 (2009)

10.101 G. Oltean, L. Nyholm, K. Edström: Galvanostatic electrodeposition of aluminium nano-rods for Li-ion three-dimensional micro-battery current collectors, Electrochim. Acta **56**, 3203–3208 (2011)

10.102 C.A. Huber, T.E. Huber, M. Sadoqi, J.A. Lubin, S. Manalis, C.B. Prater: Nanowire array composites, Science **263**, 800–802 (1994)

10.103 L. Li, X. Xu, H. Chew, X. Huang, X. Dou, S. Pan, G. Li, L. Zhang: Direct growth of Al nanowire arrays: Thermal expansion and field emission properties, J. Phys. Chem. C **112**, 5328–5332 (2008)

10.104 W.B. Jensen: The place of zinc, cadmium, and mercury in the periodic table, J. Chem. Educ. **80**, 952 (2003)

10.105 G. Wu, B. Adams, M. Tian, A. Chen: Synthesis and electrochemical study of novel Pt-decorated Ti nanowires, Electrochem. Commun. **11**, 736–739 (2009)

10.106 S. Sharma, T.I. Kamins, R.S. Williams: Diameter control of Ti-catalyzed silicon nanowires, J. Cryst. Growth **267**, 613–618 (2004)

10.107 J.S. Lehtinen: Experimental Study of Quantum Fluctuations in Titanium Nanowires in Highly Resistive Environment. M.Sc. Thesis (University of Jyväskylä, Finland 2009)

10.108 J.S. Lehtinen, T. Sajavaara, K.Y. Arutyunov, M.Y. Presnjakov, A.L. Vasiliev: Evidence of quantum phase slip effect in titanium nanowires, Phys. Rev. B **85**, 094508 (2012)

10.109 R. Spolenak, E. Zschech: *Interconnects for Microelectronics in Metal Based Thin Films for Electronics* (Wiley-VCH, Weinheim 2006)

10.110 J.A. Rogers: Stamping techniques for micro and nanofabrication: Methods and applications. In: *Springer Handbook of Nanotechnology*, ed. by B. Bhushan (Springer, Berlin, Heidelberg 2004) pp. 185–202, http://www.springerlink.com/content/ml1644666-tph405r/

10.111 Y. Zhang, H. Dai: Formation of metal nanowires on suspended single-walled carbon nanotubes, Appl. Phys. Lett. **77**, 3015–3017 (2000)

10.112 M. Ye, C.P. Grigoropoulos: Time-of-flight and emission spectroscopy study of femtosecond laser ablation of titanium, J. Appl. Phys. **89**, 5183–5190 (2001)

10.113 D. Scuderi, O. Albert, D. Moreau, P.P. Pronko, J. Etchepare: Interaction of a laser-produced plume with a second time delayed femtosecond pulse, Appl. Phys. Lett. **86**, 071502–071503 (2005)

10.114 B. Kumar, D. Yadav, R.K. Thareja: Growth dynamics of nanoparticles in laser produced plasma in liquid ambient, J. Appl. Phys. **110**, 074903–074908 (2011)

10.115 T. Sasaki, C. Liang, W.T. Nichols, Y. Shimizu, N. Koshizaki: Fabrication of oxide base nanostructures using pulsed laser ablation in aqueous solutions, Appl. Phys. A **79**, 1489–1492 (2004)

10.116 P. Jafarkhani, S. Dadras, M.J. Torkamany, J. Sabbaghzadeh: Synthesis of nanocrystalline titania in pure water by pulsed Nd:YAG Laser, Appl. Surf. Sci. **256**, 3817–3821 (2010)

10.117 A. Ayi, V. Khare, P. Strauch, J. Girard, K. Fromm, A. Taubert: On the chemical synthesis of titanium nanoparticles from ionic liquids, Monatsheft Chem. **141**, 1273–1278 (2010)

10.118 T.I. Kamins, R.S. Williams, D.P. Basile, T. Hesjedal, J.S. Harris: Ti-catalyzed Si nanowires by chemical vapor deposition: Microscopy and growth mechanisms, J. Appl. Phys. **89**, 1008–1016 (2001)

10.119 A. Corrias, G. Mountjoy, D. Gozzi, A. Latini: Multi-walled carbon nanotubes decorated with titanium nanoparticles: Synthesis and characterization, Nanotechnology **18**, 485610 (2007)

10.120 Y. Li, X. Li, Z. Deng, B. Zhou, S. Fan, J. Wang, X. Sun: From surfactant-inorganic mesostructures to tungsten nanowires, Angew. Chem. Int. Ed. **41**, 333–335 (2002)

10.121 X. Huang, Y.I. Chumlyakov, A.G. Ramirez: Defect-driven synthesis of self-assembled single crystal titanium nanowires via electrochemistry, Nanotechnology **23**, 125601 (2012)

10.122 F. Endres, Z.E. Abedin, A.Y. Saad, E.M. Moustafa, N. Borissenko, W.E. Price, G.G. Wallace, D.R. MacFarlane, P.J. Newman, A. Bund: On the electrodeposition of titanium in ionic liquids, Phys. Chem. Chem. Phys. **10**, 2189–2199 (2008)

10.123 C. Fenster, A.J. Smith, A. Abts, S. Milenkovic, A.W. Hassel: Single tungsten nanowires as pH sensitive electrodes, Electrochem. Commun. **10**, 1125–1128 (2008)

10.124 A.B.H. Tay, J.T.L. Thong: High-resolution nanowire atomic force microscope probe grown by a field-emission induced process, Appl. Phys. Lett. **84**, 5207–5209 (2004)

10.125 J.P. Singh, F. Tang, T. Karabacak, T.M. Lu, G.C. Wang: Enhanced cold field emission from ⟨100⟩ oriented β-W nanoemitters, J. Vac. Sci. Technol. B **22**, 1048–1051 (2004)

10.126 Y. Lee, C. Choi, Y. Jang, E. Kim, B. Ju, N. Min, J. Ahn: Tungsten nanowires and their field electron emission properties, Appl. Phys. Lett. **81**, 745–747 (2002)

10.127 V. Cimalla, C. Röhlig, J. Pezoldt, M. Niebelschütz, O. Ambacher, K. Brückner, M. Hein, J. Weber, S. Milenkovic, A.J. Smith, A.W. Hassel: Nanomechanics of single crystalline tungsten nanowires, J. Nanomater., 638947–638955 (2008)

10.128 L. Xiong, T. He: Synthesis and characterization of ultrafine tungsten and tungsten oxide nanoparticles by a reverse microemulsion-mediated method, Chem. Mater. **18**, 2211–2218 (2006)

10.129 V.K. Sarin: Morphological changes occurring during reduction of WO_3, J. Mater. Sci. **10**, 593–598 (1975)

10.130 Y. Chang, H. Wang, C. Chiu, D. Cheng, M. Yen, H. Chiu: Low-temperature synthesis of transition metal nanoparticles from metal complexes and organopolysilane oligomers, Chem. Mater. **14**, 4334–4338 (2002)

10.131 P.K. Sahoo, S.S. Kalyan Kamal, M. Premkumar, T. Jagadeesh Kumar, B. Sreedhar, A.K. Singh, S.K. Srivastava, K. Chandra Sekhar: Synthesis of tungsten nanoparticles by solvothermal decomposition of tungsten hexacarbonyl, Int. J. Refract. Met. Hard Mater. **27**, 784–791 (2009)

10.132 M.H. Magnusson, K. Deppert, J. Malm: Single-crystalline tungsten nanoparticles produced by thermal decomposition of tungsten hexacarbonyl, J. Mater. Res. **15**, 1564 (2000)

10.133 H. Lei, Y.J. Tang, J.J. Wei, J. Li, X.-B. Li, H.L. Shi: Synthesis of tungsten nanoparticles by sonoelectrochemistry, Ultrason. Sonochem. **14**, 81–83 (2007)

10.134 Y. Tamou, S. Tanaka: Formation and coalescence of tungsten nanoparticles under electron beam irradiation, Nanostruct. Mater. **12**, 123–126 (1999)

10.135 E. Ozawa, Y. Kawakami, T. Seto: Formation and size control of tungsten nano particles produced by Nd:YAG laser irradiation, Scr. Mater. **44**, 2279–2283 (2001)

10.136 L. Landstrom, J. Kokavecz, J. Lu, P. Heszler: Characterization and modeling of tungsten nanoparticles generated by laser-assisted chemical vapor deposition, J. Appl. Phys. **95**, 4408–4414 (2004)

10.137 Z.Q. Liu, K. Mitsuishi, K. Furuya: Features of self-supporting tungsten nanowire deposited with high-energy electrons, J. Appl. Phys. **96**, 619–623 (2004)

10.138 Z.Q. Liu, K. Mitsuishi, K. Furuya: The growth behavior of self-standing tungsten tips fabricated by electron-beam-induced deposition using 200 keV electrons, J. Appl. Phys. **96**, 3983–3986 (2004)

10.139 S. Vaddiraju, H. Chandrasekaran, M.K. Sunkara: Vapor phase synthesis of tungsten nanowires, J. Am. Chem. Soc. **125**, 10792–10793 (2003)

10.140 A.W. Hassel, S. Milenkovic, A.J. Smith: Large scale synthesis of single crystalline tungsten nanowires with extreme aspect ratios, Phys. Status Solidi (a) **207**, 858–863 (2010)

10.141 J.T.L. Thong, C.H. Oon, M. Yeadon, W.D. Zhang: Field-emission induced growth of nanowires, Appl. Phys. Lett. **81**, 4823–4825 (2002)

10.142 S. Wang, Y. He, J. Zou, Y. Jiang, J. Xu, B. Huang, C.T. Liu, P.K. Liaw: Synthesis of single-crystalline tungsten nanowires by nickel-catalyzed vapor-phase method at 850 °C, J. Cryst. Growth **306**, 433–436 (2007)

10.143 E. Redel, R. Thomann, C. Janiak: Use of ionic liquids (ILs) for the IL-anion size-dependent formation of Cr, Mo and W nanoparticles from metal carbonyl $M(CO)_6$ precursors, Chem. Commun., 1789–1791 (2008)

10.144 J.A. Rodriguez, J. Dvorak, T. Jirsak, J. Hrbek: Formation of Mo and MoS_x nanoparticles on Au(1 1 1) from $Mo(CO)_6$ and S_2 precursors: Electronic and chemical properties, Surf. Sci. **490**, 315–326 (2001)

10.145 C. Vollmer, E. Redel, K. Abu-Shandi, R. Thomann, H. Manyar, C. Hardacre, C. Janiak: Microwave irradiation for the facile synthesis of transition-metal nanoparticles (NPs) in ionic liquids (ILs) from metal-carbonyl precursors and Ru-, Rh-, and Ir-NP/IL dispersions as biphasic liquid-liquid hydrogenation nanocatalysts for cyclohexene, Chem. Eur. J. **16**, 3849–3858 (2010)

10.146 D.V. Potapenko, J.M. Horn, R.J. Beuhler, Z. Song, M.G. White: Reactivity studies with gold-supported molybdenum nanoparticles, Surf. Sci. **574**, 244–258 (2005)

10.147 P. Liu, J.A. Rodriguez, J.T. Muckerman, J. Hrbek: The deposition of Mo nanoparticles on Au(111) from

a $Mo(CO)_6$ precursor: Effects of CO on Mo–Au intermixing, Surf. Sci. **530**, L313–L321 (2003)
10.148 S. Mitra, K. Sridharan, J. Unnam, K. Ghosh: Synthesis of nanometal oxides and nanometals using hot-wire and thermal CVD, Thin Solid Films **516**, 798–802 (2008)
10.149 M. Komarneni, E. Kadossov, J. Justin, M. Lu, U. Burghaus: Adsorption of thiophene on silica-supported Mo clusters, Surf. Sci. **604**, 1221–1229 (2010)
10.150 Z. Jiang, W. Huang, Z. Zhang, H. Zhao, D. Tan, X. Bao: Multiple coordination of CO on molybdenum nanoparticles: Evidence for intermediate $Mo_x(CO)_y$ species by XPS and UPS, J. Phys. Chem. B **110**, 26105–26113 (2006)
10.151 L. Bugyi, R. Németh: Characterization of Rh, Mo and Rh–Mo particles formed on TiO_2(110) surface: A TDS, AES and RAIRS study, Surf. Sci. **605**, 808–817 (2011)
10.152 M. Chhowalla, G.A.J. Amaratunga: Thin films of fullerene-like MoS_2 nanoparticles with ultra-low friction and wear, Nature **407**, 164–167 (2000)
10.153 J.M. Martin, C. Donnet, T. Le Mogne, T. Epicier: Superlubricity of molybdenum disulphide, Phys. Rev. B **48**, 10583–10586 (1993)
10.154 L.W. Vernon, J.T. Richardson: Hydrogenolysis of thiophene, US Patent 19 (1961)
10.155 F.C. Riddick Jr., B. Peralta: Hydrodesulfurization of oil feedstock with presulfided catalyst, US Patent 22 (1980)
10.156 G.B. Brignac, J. Kociscin, C.A. McKnight: Catalyst activation method for selective cat naphtha hydrodesulfurization, US Patent 6 (2001)
10.157 A. Tuxen, J. Kibsgaard, H. Gobel, E. Laegsgaard, H. Topsoe, J.V. Lauritsen, F. Besenbacher: Size threshold in the dibenzothiophene adsorption on MoS_2 nanoclusters, ACS Nano **4**, 4677–4682 (2010)
10.158 J. Chen, S. Li, Q. Xu, K. Tanaka: Synthesis of open-ended MoS_2 nanotubes and the application as the catalyst of methanation, Chem. Commun., 1722–1723 (2002)
10.159 T.F. Jaramillo, K.P. Jørgensen, J. Bonde, J.H. Nielsen, S. Horch, I. Chorkendorff: Identification of active edge sites for electrochemical H_2 evolution from MoS_2 nanocatalysts, Science **317**, 100–102 (2007)
10.160 M.L. Tang, D.C. Grauer, B. Lassalle-Kaiser, V.K. Yachandra, L. Amirav, J.R. Long, J. Yano, A.P. Alivisatos: Structural and electronic study of an amorphous MoS_3 hydrogen-generation catalyst on a quantum-controlled photosensitizer, Angew. Chem. Int. Ed. **50**, 10203–10207 (2011)
10.161 L.X. Song, M. Wang, S.Z. Pan, J. Yang, J. Chen, J. Yang: Molybdenum oxide nanoparticles: Preparation, characterization, and application in heterogeneous catalysis, J. Mater. Chem. **21**, 7982–7989 (2011)
10.162 R. Liang, H. Cao, D. Qian: MoO_3 nanowires as electrochemical pseudocapacitor materials, Chem. Commun. **47**, 10305–10307 (2011)
10.163 S. Lee, Y. Kim, R. Deshpande, P.A. Parilla, E. Whitney, D.T. Gillaspie, K.M. Jones, A.H. Mahan, S. Zhang, A.C. Dillon: Reversible lithium-ion insertion in molybdenum oxide nanoparticles, Adv. Mater. **20**, 3627–3632 (2008)
10.164 R. Tenne, M. Remškar, A. Enyashin, G. Seifert: Inorganic nanotubes and fullerene-like structures (IF). In: *Carbon Nanotubes*, Topics in Applied Physics Ser., Vol. 111, ed. by J. Ado, G. Dresselhaus, M.S. Dresselhaus, S. Mildred (Springer, Berlin, Heidelberg 2008) pp. 631–671
10.165 T. Matsumoto, Y. Nagashima, T. Yamazaki, J. Nakamura: Fuel cell anode composed of Mo_2C catalyst and carbon nanotube electrodes, Electrochem. Solid-State Lett. **9**, A160–A162 (2006)
10.166 B. Radisavljevic, M.B. Whitwick, A. Kis: Integrated circuits and logic operations based on single-layer MoS_2, ACS Nano **5**, 9934–9938 (2011)
10.167 K. Lee, H. Kim, M. Lotya, J.N. Coleman, G. Kim, G.S. Duesberg: Electrical characteristics of molybdenum disulfide flakes produced by liquid exfoliation, Adv. Mater. **23**, 4178–4182 (2011)
10.168 S. Wu, Z. Zeng, Q. He, Z. Wang, S.J. Wang, Y. Du, Z. Yin, X. Sun, W. Chen, H. Zhang: Electrochemically reduced single-layer MoS_2 nanosheets: Characterization, properties, and sensing applications, Small **8**, 2264–2270 (2012)
10.169 A. Fukunaga, S. Chu, M.E. McHenry: Synthesis, structure, and superconducting properties of tantalum carbide nanorods and nanoparticles, J. Mater. Res. **13**, 2465–2471 (1998)
10.170 C.M. Lieber, E. Wong: Preparation of carbide nanorods, US Patent 7 (1999)
10.171 K.Y. Chick, M. Nath, B.A. Parkinson: TaS_2 nanoplatelets produced by laser ablation, J. Mater. Res. **21**, 1243–1247 (2006)
10.172 C.W. Dunnill, H.K. Edwards, P.D. Brown, D.H. Gregory: Single-step synthesis and surface-assisted growth of superconducting TaS_2 nanowires, Angew. Chem. Int. Ed. **45**, 7060–7063 (2006)
10.173 X. Wu, Y. Tao, Y. Hu, Y. Song, Z. Hu, J. Zhu, L. Dong: Tantalum disulfide nanobelts: Preparation, superconductivity and field emission, Nanotechnology **17**, 201 (2006)
10.174 H. El-Sayed, V.I. Birss: Controlled growth and monitoring of tantalum oxide nanostructures, Nanoscale **2**, 793–798 (2010)
10.175 X. Feng, T.J. LaTempa, J.I. Basham, G.K. Mor, O.K. Varghese, C.A. Grimes: Ta_3N_5 nanotube arrays for visible light water photoelectrolysis, Nano Lett. **10**, 948–952 (2010)
10.176 M. Tabata, K. Maeda, M. Higashi, D. Lu, T. Takata, R. Abe, K. Domen: Modified Ta_3N_5 powder as a photocatalyst for O_2 evolution in a two-step water splitting system with an iodate/iodide shuttle re-

dox mediator under visible light, Langmuir **26**, 9161–9165 (2010)
10.177 A. Engel, A. Aeschbacher, K. Inderbitzin, A. Schilling, K. Ilin, M. Hofherr, M. Siegel, A. Semenov, H.-W. Hubers: Tantalum nitride superconducting single-photon detectors with low cut-off energy, Appl. Phys. Lett. **100**, 062601–062603 (2012)
10.178 S. Sato, T. Morikawa, S. Saeki, T. Kajino, T. Motohiro: Visible-light-induced selective CO_2 reduction utilizing a ruthenium complex electrocatalyst linked to a p-type nitrogen-doped Ta_2O_5 semiconductor, Angew. Chem. Int. Ed. **49**, 5101–5105 (2010)
10.179 M. Higashi, K. Domen, R. Abe: Highly stable water splitting on oxynitride TaON photoanode system under visible light irradiation, J. Am. Chem. Soc. **134**, 6968–6971 (2012)
10.180 J.M. Mativetsky, S. Fostner, S.A. Burke, P. Grutter: High-resolution investigation of metal nanoparticle growth on an insulating surface, Phys. Rev. B **80**, 045430 (2009)
10.181 J. Barr, R. Axelbaum, M. Macias: Processing salt-encapsulated tantalum nanoparticles for high purity, ultra high surface area applications, J. Nanopart. Res. **8**, 11–22 (2006)
10.182 Y. Wang, Z. Cui, Z. Zhang: Synthesis and phase structure of tantalum nanoparticles, Mater. Lett. **58**, 3017–3020 (2004)
10.183 J. Walter, H. Shioyama, Y. Sawada: The generation of nanometer-size tantalum particles in a graphite host lattice, Carbon **37**, 41–45 (1999)
10.184 I.S. Suzuki, M. Suzuki, J. Walter: Superconductivity and magnetism in tantalum–graphite multilayers based on natural graphite, Solid State Commun. **118**, 523–527 (2001)
10.185 R.L. Axelbaum, D.P. DuFaux, L.J. Rosen: Method and apparatus for producing high purity and unagglomerated submicron particles, US Patent 30 (1995)
10.186 M. Law, L.E. Greene, J.C. Johnson, R. Saykally, P. Yang: Nanowire dye-sensitized solar cells, Nat. Mater. **4**, 455–459 (2005)
10.187 B. Liu, H.C. Zeng: Mesoscale organization of CuO nanoribbons: Formation of "Dandelions", J. Am. Chem. Soc. **126**, 8124–8125 (2004)
10.188 B.O. Dabbousi, J. Rodriguez-Viejo, F.V. Mikulec, J.R. Heine, H. Mattoussi, R. Ober, K.F. Jensen, M.G. Bawendi: (CdSe)ZnS core-shell quantum dots: Synthesis and characterization of a size series of highly luminescent nanocrystallites, J. Phys. Chem. B **101**, 9463–9475 (1997)
10.189 P.X. Gao, Z.L. Wang: Nanoarchitectures of semiconducting and piezoelectric zinc oxide, J. Appl. Phys. **97**, 044304–044307 (2005)
10.190 Y. Wang, L. Zhang, G. Meng, C. Liang, G. Wang, S. Sun: Zn nanobelts: A new quasi one-dimensional metal nanostructure, Chem. Commun., 2632–2633 (2001)
10.191 X.S. Peng, L.D. Zhang, G.W. Meng, X.Y. Yuan, Y. Lin, Y.T. Tian: Synthesis of Zn nanofibres through simple thermal vapour-phase deposition, J. Phys. D **36**, L35 (2003)
10.192 J. Wu, S. Liu, C. Wu, K. Chen, L. Chen: Heterostructures of ZnO–Zn coaxial nanocables and ZnO nanotubes, Appl. Phys. Lett. **81**, 1312–1314 (2002)
10.193 J.Q. Hu, Q. Li, X.M. Meng, C.S. Lee, S.T. Lee: Thermal reduction route to the fabrication of coaxial Zn/ZnO nanocables and ZnO nanotubes, Chem. Mater. **15**, 305–308 (2003)
10.194 Y. Yan, P. Liu, M.J. Romero, M. Al-Jassim: Formation of metallic zinc nanowires, J. Appl. Phys. **93**, 4807–4809 (2003)
10.195 S.C. Singh, R. Gopal: Zinc nanoparticles in solution by laser ablation technique, Bull. Mater. Sci. **30**, 291–293 (2007)
10.196 S.C. Singh, R.K. Swarnkar, R. Gopa: Zn/ZnO core/shell nanoparticles synthesized by laser ablation in aqueous environment: Optical and structural characterizations, Bull. Mater. Sci. **33**, 21–26 (2010)
10.197 J. Wang, M. Tian, N. Kumar, T.E. Mallouk: Controllable template synthesis of superconducting Zn nanowires with different microstructures by electrochemical deposition, Nano Lett. **5**, 1247–1253 (2005)
10.198 G.G. Jernigan, G.A. Somorjai: Carbon monoxide oxidation over three different oxidation states of copper: Metallic copper, copper (I) oxide, and copper (II) oxide – A surface science and kinetic study, J. Catal. **147**, 567–577 (1994)
10.199 Y. Zhang, W. Huang, S.E. Habas, J.N. Kuhn, M.E. Grass, Y. Yamada, P. Yang, G.A. Somorjai: Near-monodisperse NiCu bimetallic nanocrystals of variable composition: Controlled synthesis and catalytic activity for H_2 generation, J. Phys. Chem. C **112**, 12092–12095 (2008)
10.200 R.L. Keiski, O. Desponds, Y. Chang, G.A. Somorjai: Kinetics of the water-gas shift reaction over several alkane activation and water-gas shift catalysts, Appl. Catal. A **101**, 317–338 (1993)
10.201 G.A. Somorjai, R.L. York, D. Butcher, J.Y. Park: The evolution of model catalytic systems; studies of structure, bonding and dynamics from single crystal metal surfaces to nanoparticles, and from low pressure ($<10^{-3}$ Torr) to high pressure ($>10^{-3}$ Torr) to liquid interfaces, Phys. Chem. Chem. Phys. **9**, 3500 (2007)
10.202 J.A. Rodriguez, P. Liu, J. Hrbek, J. Evans, M. Pérez: Water gas shift reaction on Cu and Au nanoparticles supported on $CeO_2(111)$ and $ZnO(000\bar{1})$: Intrinsic activity and importance of support interactions, Angew. Chem. Int. Ed. **46**, 1329–1332 (2007)
10.203 A.A. Gokhale, J.A. Dumesic, M. Mavrikakis: On the mechanism of low-temperature water gas shift re-

action on copper, J. Am. Chem. Soc. **130**, 1402–1414 (2008)
10.204 T. Ressler, B.L. Kniep, I. Kasatkin, R. Schlögl: The microstructure of copper zinc oxide catalysts: Bridging the materials gap, Angew. Chem. Int. Ed. **44**, 4704–4707 (2005)
10.205 S. Vukojevic, O. Trapp, J. Grunwaldt, C. Kiener, F. Schüth: Quasi-homogeneous methanol synthesis over highly active copper nanoparticles, Angew. Chem. Int. Ed. **44**, 7978–7981 (2005)
10.206 P.L. Hansen, J.B. Wagner, S. Helveg, J. Rostrup-Nielsen, B.S. Clausen, H. Topse: Atom-resolved imaging of dynamic shape changes in supported copper nanocrystals, Science **295**, 2053–2055 (2002)
10.207 M.K. Schröter, L. Khodeir, M.W.E. van der Berg, T. Hikov, M. Cokoja, S. Miao, W. Grünert, M. Muhler, R.A. Fischer: A colloidal ZnO/Cu nanocatalyst for methanol synthesis, Chem. Commun., 2498–2500 (2006)
10.208 A.A. Ponce, K.J. Klabunde: Chemical and catalytic activity of copper nanoparticles prepared via metal vapor synthesis, J. Mol. Catal. A **225**, 1–6 (2005)
10.209 V.T. Renard, M. Jublot, P. Gergaud, P. Cherns, D. Rouchon, A. Chabli, V. Jousseaume: Catalyst preparation for CMOS-compatible silicon nanowire synthesis, Nat. Nano **4**, 654–657 (2009)
10.210 A.A. Setlur, J.M. Lauerhaas, J.Y. Dai, R.P.H. Chang: A method for synthesizing large quantities of carbon nanotubes and encapsulated copper nanowires, Appl. Phys. Lett. **69**, 345 (1996)
10.211 Z. Liu, Y. Bando: A novel method for preparing copper nanorods and nanowires, Adv. Mater. **15**, 303–305 (2003)
10.212 R.K. Swarnkar, S.C. Singh, R. Gopal: Effect of aging on copper nanoparticles synthesized by pulsed laserablation in water: Structural and optical characterizations, Bull. Mater. Sci. **34**, 1363–1369 (2011)
10.213 N. Bärsch, J. Jakobi, S. Weiler, S. Barcikowski: Pure colloidal metal and ceramic nanoparticles from high-power picosecond laser ablation in water and acetone, Nanotechnology **20**, 445603 (2009)
10.214 K. Murai, Y. Tokoi, H. Suematsu, W. Jiang, K. Yatsui, K. Niihara: Particle size controllability of ambient gas species for copper nanoparticles prepared by pulsed wire discharge, Jpn. J. Appl. Phys. **47**, 3726 (2008)
10.215 G. Vitulli, M. Bernini, S. Bertozzi, E. Pitzalis, P. Salvadori, S. Coluccia, G. Martra: Nanoscale copper particles derived from solvated Cu atoms in the activation of molecular oxygen, Chem. Mater. **14**, 1183–1186 (2002)
10.216 Y.H. Kim, D.K. Lee, B.G. Jo, J.H. Jeong, Y.S. Kang: Synthesis of oleate capped Cu nanoparticles by thermal decomposition, Colloids Surf. Physicochem. Eng. Asp. **284–285**, 364–368 (2006)
10.217 M.E. Toimil Molares, V. Buschmann, D. Dobrev, R. Neumann, R. Scholz, I.U. Schuchert, J. Vetter: Single-crystalline copper nanowires produced by electrochemical deposition in polymeric ion track membranes, Adv. Mater. **13**, 62 (2001)
10.218 M.E. Toimil Molares, E.M. Hohberger, C. Schaeflein, R. Blick, H.R. Neumann, C. Trautmann: Electrical characterization of electrochemically grown single copper nanowires, Appl. Phys. Lett. **82**, 2139 (2003)
10.219 H. Choi, S. Park: Seedless growth of free-standing copper nanowires by chemical vapor deposition, J. Am. Chem. Soc. **126**, 6248 (2004)
10.220 M. Mohl, P. Pusztai, A. Kukovecz, Z. Konya, J. Kukkola, K. Kordas, R. Vajtai, P.M. Ajayan: Low-temperature large-scale synthesis and electrical testing of ultralong copper nanowires, Langmuir **26**, 16496–16502 (2010)
10.221 Z. Liu, Y. Yang, J. Liang, Z. Hu, S. Li, S. Peng, Y. Qian: Synthesis of copper nanowires via a complex-surfactant-assisted hydrothermal reduction process, J. Phys. Chem. B **107**, 12658 (2003)
10.222 N.J. Gerein, J.A. Haber: Effect of AC electrodeposition conditions on the growth of high aspect ratio copper nanowires in porous aluminum oxide templates, J. Phys. Chem. B **109**, 17372 (2005)
10.223 M. Yen, C. Chiu, C. Hsia, F. Chen, J. Kai, C. Lee, H. Chiu: Synthesis of cable-like copper nanowires, Adv. Mater. **15**, 235 (2003)
10.224 M. Pileni: The role of soft colloidal templates in controlling the size and shape of inorganic nanocrystals, Nat. Mater. **2**, 145 (2003)
10.225 A. Filankembo, M.P. Pileni: Is the template of self-colloidal assemblies the only factor that controls nanocrystal shapes?, J. Phys. Chem. B **104**, 5865 (2000)
10.226 A.C. Curtis, D.G. Duff, P.P. Edwards, D.A. Jefferson, B.F.G. Johnson, A.I. Kirkland, A.S. Wallace: A morphology-selective copper organosol, Angew. Chem. Int. Ed. **27**, 1530–1533 (1988)
10.227 D. Mott, J. Galkowski, L. Wang, J. Luo, C. Zhong: Synthesis of size-controlled and shaped copper nanoparticles, Langmuir **23**, 5740–5745 (2007)
10.228 Y. Chang, M.L. Lye, H.C. Zeng: Large-scale synthesis of high-quality ultralong copper nanowires, Langmuir **21**, 3746–3748 (2005)
10.229 I. Lisiecki: Size, shape, and structural control of metallic nanocrystals, J. Phys. Chem. B **109**, 12231–12244 (2005)
10.230 M. Jin, G. He, H. Zhang, J. Zeng, Z. Xie, Y. Xia: Shape-controlled synthesis of copper nanocrystals in an aqueous solution with glucose as a reducing agent and hexadecylamine as a capping agent, Angew. Chem. Int. Ed. **50**, 10560–10564 (2011)
10.231 Y. Shi, H. Li, L. Chen, X. Huang: Obtaining ultralong copper nanowires via a hydrothermal process, Sci. Technol. Adv. Mater. **6**, 761 (2005)

10.232 M. Mohl, D. Dobo, A. Kukovecz, Z. Konya, K. Kordas, J. Wei, R. Vajtai, P.M. Ajayan: Formation of CuPd and CuPt bimetallic nanotubes by galvanic replacement reaction, J. Phys. Chem. C **115**, 9403–9409 (2011)
10.233 Y. Wang, P. Chen, M. Liu: Synthesis of well-defined copper nanocubes by a one-pot solution process, Nanotechnology **17**, 6000 (2006)
10.234 G. Zhou, M. Lu, Z. Yang: Aqueous synthesis of copper nanocubes and bimetallic copper/palladium core-shell nanostructures, Langmuir **22**, 5900–5903 (2006)
10.235 M.H. Kim, B. Lim, E.P. Lee, Y. Xia: Polyol synthesis of Cu_2O nanoparticles: Use of chloride to promote the formation of a cubic morphology, J. Mater. Chem. **18**, 4069–4073 (2008)